AGU100 ADVANCING EARTH AND SPACE SCIENCE

JGR

Journal of Geophysical Research: Space Physics

RESEARCH ARTICLE
10.1029/2018JA025952

Special Section:
The Earth's Magnetosphere: New Tools, New Thinking, New Results

On the Forecast Horizon of Magnetospheric Dynamics: A Scale-to-Scale Approach

Giuseppe Consolini[1], Tommaso Alberti[1], and Paola De Michelis[2]

[1]INAF-Istituto di Astrofisica e Planetologia Spaziali, Roma, Italy, [2]Istituto Nazionale di Geofisica e Vulcanologia, Roma, Italy

Key Points:
- A dynamical system approach is used to describe magnetospheric dynamics as seen by scale-to-scale fluctuations of SYM-H and AE indices
- Correlation dimension D_2 and Kolmogorov entropy K_2 are scale-dependent but independent on the phases of the solar activity cycle
- Forecast horizon is very small (approx. 2 min) for short-timescale fluctuations, which are crucial for Space Weather purposes

Correspondence to:
G. Consolini,
giuseppe.consolini@inaf.it

Citation:
Consolini, G., Alberti, T., & De Michelis, P. (2018). On the forecast horizon of magnetospheric dynamics: A scale-to-scale approach. *Journal of Geophysical Research: Space Physics*, *123*, 9065–9077. https://doi.org/10.1029/2018JA025952

Received 31 JUL 2018
Accepted 12 OCT 2018
Accepted article online 17 OCT 2018
Published online 8 NOV 2018

Abstract The Earth's magnetosphere is characterized by a complex dynamics resulting from the interaction of different multiscale processes which can be both directly driven/triggered by the interplanetary magnetic field and the solar wind, and due to internal processes of the magnetosphere. Recently, Alberti et al. (2017, https://doi.org/10.1002/2016JA023175) have shown that the fluctuations at distinct timescales of some geomagnetic indices differently respond to interplanetary changes during geomagnetic storms. In detail, using an information theory based approach it has been shown that geomagnetic indices fluctuations occurring at long timescales (typically longer than 200 min) are correlated with physical quantities characterizing the changes of the interplanetary conditions, while the short timescale ones (typically shorter than 200 min) do not seem to be directly related to the same physical quantities. The aim of this work is to identify the nature and character of the scale-to-scale fluctuations of two geomagnetic indices, AE and SYM-H, capable of monitoring different geomagnetic current systems related to the occurrence of geomagnetic storms and substorms. By applying the theory of dynamical systems, we investigate the scale-to-scale correlation dimension D_2 and the Kolmogorov entropy K_2 showing the occurrence of a topological phase transition phenomenon between long and short-timescale fluctuations. Furthermore, our results clearly show that the forecast horizon of fluctuations occurring at timescales shorter than 200 min dramatically decreases down to ~2 min. The consequences of this result in the framework of Space Weather forecasting is briefly outlined and discussed.

1. Introduction

The dynamics of the Earth's magnetosphere in response to the changes of the solar wind and of the interplanetary orientations is very complex, showing phenomena that occur on a wide range of temporal and spatial scales. This complex dynamics, which is the results of the interplay of the solar wind external driving and the processes taking place inside the different regions of the Earth's magnetosphere, manifests in the bursty and intermittent character of the geomagnetic indices (AE indices, Sym-H, etc.), which provide information on the overall magnetospheric dynamics.

In the early 1990s several studies analyzed the possibility that the highly intermittent and complex dynamics of the Earth's magnetosphere might be due to an inherent nonlinear character of the magnetospheric response to solar wind changes (Tsurutani et al., 1990) and/or to the occurrence of low-dimensional chaos (Baker et al., 1990; Klimas et al., 1996; Sharma, 1995; Vassiliadis et al., 1990). Later it was realized that the dynamics of the Earth's magnetosphere contained elements that could not be simply explained in terms of a low-dimensional chaos, but that were proper of dynamical systems near a critical point and/or of nonequilibrium phase transitions (Balasis et al., 2006; Consolini, 2002, 1997; Klimas et al., 1996; Lui et al., 2000; Sharma et al., 2001; Sitnov et al., 2000; Uritsky et al., 2002; Uritsky & Pudovkin, 1998).

Nowadays, it is known that the complex dynamics of the Earth's magnetosphere manifests in several properties such as, for example, the scale-invariant features, which characterize both the time series of geomagnetic indices and the statistical properties of the high-latitude energy deposition during the magnetic substorms (Consolini, 2002; Uritsky et al., 2002), the turbulent character of the plasma in the magnetotail central plasma sheet (CPS; see, e.g., Borovsky et al., 1997; Vörös et al., 2006, and references therein), the multiscale features of magnetosphere and magnetotail dynamics (Vörös et al., 2004), the Brownian character of the dynamics of some geomagnetic indices (see e.g., Consolini, 2018, Wei et al., 2004, and references therein). All the above-mentioned properties of the magnetospheric dynamics have a great impact on the capability to forecast the geomagnetic response to solar wind changes. The inherent multiscale and near criticality character

of the magnetospheric dynamics can give rise to some critical issues in the right forecast of the geomagnetic response to solar wind changes, especially at the short timescales, that is, at timescales of the order of few minutes that are strongly affected by the above phenomena. This may be one of the reasons for some difficulties encountered by machine-learning and artificial neural networks (ANNs) approaches, Burtons models, and regression analysis to forecast the short-timescale variations of the geomagnetic indices. On the other hand, the correct estimation and forecasting of short-timescale fluctuations is extremely important in the framework of Space Weather studies being the fast and large variations of geomagnetic field the most effective and dangerous for the anthropic systems.

Pallocchia et al. (2008) clearly showed how short-timescale forecasting of AE index based on L1 WIND interplanetary magnetic field and plasma data by using ANN algorithms was extremely difficult. They were not capable of correctly reproducing the AE index variations occurring at timescales shorter than 60 min. The failure of forecasting capability at short timescale can be explained by considering that the magnetospheric dynamics comprises both the internal dynamics and the solar wind directly driven/triggered processes which act on different timescales. In a recent paper, using a science system approach based on information theory, Alberti et al. (2017) have clearly shown how the correlation between the external drivers and the magnetospheric response, monitored by AE index and SYM-H index, is poorly significantly at timescales below 200 min during some geomagnetic storms. This result supports the old ideas and findings according to which a better forecasting of the magnetospheric response requires the knowledge of some proxies capable of quantifying the internal magnetotail state (Takalo & Timonen, 1997), and that at shorter timescales the magnetospheric dynamics shows features that are independent from those of the solar wind (Uritsky et al., 2001). On the other hand, geomagnetic indices variations on longer timescales show a good correlation with the changes of solar wind parameters and interplanetary magnetic field. This is also supported by a recent study based on the canonical correlation analysis of combined solar wind and geomagnetic index data by Borovsky (2013), that allows us to clearly unveil the existence of nontrivial correlation patterns between the external drivers and the magnetospheric response by using 1 hr resolution data.

The aim of this work is to better characterize the differences between the short and long-timescale fluctuations observed in the AE and SYM-H geomagnetic indices in order to unveil the possible different magnetospheric dynamic characters at different timescales. We investigate the scale-to-scale forecast horizon by combining two different analysis method, the Empirical Mode Decomposition (EMD; Huang et al., 1998) and the traditional correlation dimension D_2 and K_2 entropy analysis (Grassberger & Procaccia, 1983; Takens, 1981), already widely used in the past to quantify the overall chaotic nature of the geomagnetic response during magnetic substorms (Vassiliadis et al., 1990). The aim is both to analyze the dependence of the timescales of the fluctuations from the correlation dimension D_2 and the corresponding forecast horizon, estimated by using the K_2 entropy analysis, and to explore the possible emergence of different dynamical regimes. We believe that the overall magnetospheric dynamics as monitored by geomagnetic indices is the result of competing processes occurring at different timescales so that the previous results by Vassiliadis et al. (1990) on a fractal correlation dimension $D_2 \simeq 3.6$ and a Kolmogorov entropy $K_2 < 0.2$ min^{-1} have to be considered as average features. We expect that there should be a sort of topological transition accompanied by a change of the correlation dimension D_2 with the fluctuation timescale (Chang et al., 1992, 2003).

The paper is organized as follows: section 2 is devoted to the description of data and methods of analysis; section 3 illustrates the results and their discussion; section 4 presents the conclusions and their relevance in the framework of Space Weather studies.

2. Data and Methods

2.1. Geomagnetic Indices

The overall magnetospheric dynamics can be described and monitored by using different geomagnetic indices, which are generally proxies of the changes of both magnetospheric and ionospheric current systems. Here we put our attention on two specific geomagnetic indices: SYM-H and AE. The low-latitude SYM-H index, introduced by Iyemori (1990), is widely used to describe geomagnetic variations at mid-low latitudes in terms of symmetric disturbances for the horizontal component of the geomagnetic field as measured over a set of quasi-equatorial distributed geomagnetic observatories. This index, which can be considered a high-resolution version of the most famous Dst index (Wanliss & Showalter, 2006), has the advantage of having a time resolution of 1 min, in respect to the 1 hr resolution of Dst, allowing a better investiga-

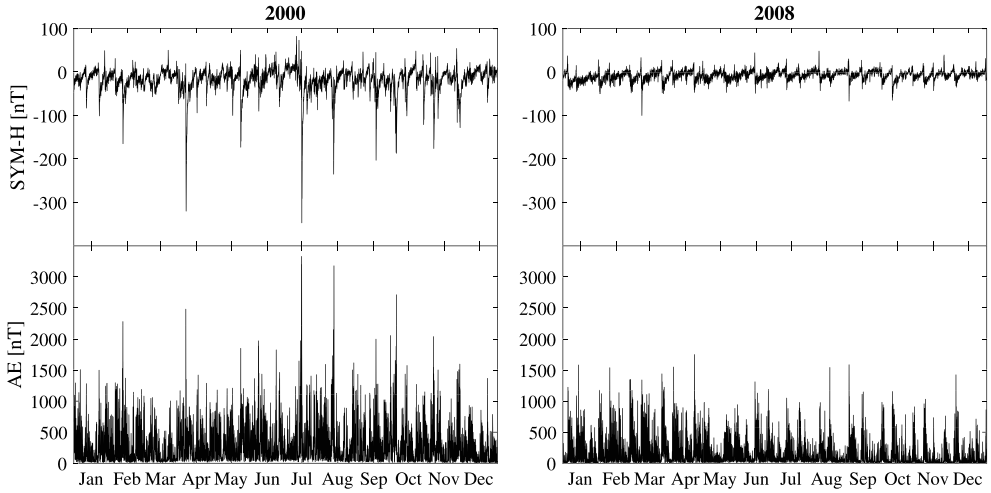

Figure 1. Time behavior of the geomagnetic indices for the solar maximum (left panels) and minimum (right panels) selected time intervals. An intense geomagnetic activity is clearly visible to occur during the year 2000, which corresponds with the solar maximum phase of the solar cycle 23.

tion of short-timescale geomagnetic variations due to changes of the solar wind dynamic pressure and magnetospheric ring current.

The Auroral Electroject (AE) index (T. Davis & Sugiura, 1966), derived from ground-based measurements of the geomagnetic field horizontal component (H) at 12 high-latitude geomagnetic observatories and characterized by a 1 min time resolution, can be used to investigate high-latitude geomagnetic variations of the electrojet currents flowing in the polar ionosphere during geomagnetic substorms, being indeed an estimate of the overall horizontal current strength flowing in the auroral regions. Specifically, AE index gives a measure of the overall activity of the auroral electrojets, providing an indirect measurement of large-scale energy outflow from the magnetosphere toward the high-latitude ionosphere and of the ionospheric energy losses (Ahn et al., 1983). This index has been widely used in the past to study the overall geomagnetic response during geomagnetic substorms and to investigate the emergence of complexity and criticality in the magnetospheric dynamics (see, e.g., Baker et al., 1990; Consolini et al., 1996; Consolini, 1997; Klimas et al., 1996; Uritsky & Pudovkin, 1998; Vassiliadis et al., 1990, and references therein)

Geomagnetic indices time series, used in this work, have been freely retrieved at OMNIWeb-database website (http://omniweb.gsfc.nasa.gov) and consist of two 1 year length different periods relative to the maximum and minimum phases of the solar cycle 23. In detail, the two different data set cover the time intervals from 1 January to 31 December 2000 (solar maximum) and from 1 January to 31 December 2008 (solar minimum), respectively, during which the sunspot number (SSN) reached its maximum and minimum values (i.e., SSN = 173.9 $\pm$ 10.1 for the year 2000, SSN = 4.2 $\pm$ 2.5 for the year 2008, respectively, see http://sidc.be/silso/datafiles). The choice of two different time intervals corresponding to different solar cycle phases and different levels of the geomagnetic activity is done in order to investigate the possible dependence of the scale-to-scale dynamics on the solar activity level. Figure 1 reports the time series of the considered quantities (SYM-H and AE indices) for the selected periods according to the solar maximum and minimum phases, respectively.

The reported time series clearly evidence a different behavior, in terms of amplitude variations, of both geomagnetic indices, due to the different solar activity levels. During the solar maximum phase the two geomagnetic indices exhibit larger excursions than during the solar minimum phase. A minimum (maximum) value of SYM-H (AE) is found about ~ -347 nT ($\sim$3330 nT) in correspondence of the famous Bastille Day geomagnetic storm (14 July 2000), while during the solar minimum phase the minimum (maximum) value is ~ -100 nT ($\sim$1750 nT), which was recorded on 8 March 2008. Moreover, another interesting feature is that the variance is completely different between the two periods, being the ratio $\sigma^2_{2000}/\sigma^2_{2008} \sim 7$ and $\sigma^2_{2000}/\sigma^2_{2008} \sim 2.5$ for SYM-H and AE, respectively. This is again the evidence of a different level of geomagnetic activity in the different solar phases.

2.2. The Hilbert-Huang Transform

Actual times series, which represent the evolution of some quantities of a natural systems, are often characterized by a high degree of nonstationarity and nonlinearity such that, in order to avoid misleading results, it is necessary to require some minimal assumptions. In this framework a useful method to treat systems displaying these features is the EMD method, the first step of the Hilbert-Huang transform (HHT; Huang et al., 1998). This last method, HHT, which consists of the EMD and the Hilbert spectral analysis, has an empirical fully adaptive character since no pre-fixed decomposition basis is chosen, and allows to extract local nonstationary features of time series under analysis by introducing the novel concept of instantaneous frequency (Huang et al., 2009). In the following we briefly summarize the general features of the method (detailed descriptions can be found in our previous works, e.g., Alberti et al., 2017; De Michelis et al., 2012).

The EMD decomposes a time series $y(t)$ (here the geomagnetic indices time series, i.e., $y(t) = \text{SYM-H}(t)$ or $y(t) = \text{AE}(t)$) into a finite number of local intrinsic oscillating functions $c_k(t)$, known as intrinsic mode functions (IMFs) or empirical modes, and a residue (nonoscillating) function $r(t)$, so that one can write $y(t)$ as

$$y(t) = \sum_{k=1}^{N} c_k(t) + r(t). \tag{1}$$

Each empirical mode is obtained via an iterative procedure, known as sifting process, which is based on the local features of time series (number of local extrema and zero crossings, upper and lower envelopes) and consists of a finite number of iteration steps. In particular, the IMFs result to be zero-mean, locally orthogonal, oscillating/fluctuating signals, each of which is characterized by a limited range of scales (see, e.g., Huang et al., 1998, for more details about IMF definition and stopping criteria for the sifting process). The fact that IMFs are zero-mean oscillating signals, allows a correct application of the Hilbert Transform. Indeed, the main novelty of the HHT approach is the introduction of the concept of instantaneous frequency, instead of (pre-)fixed constant frequency-based methods (e.g., Fourier transform, Wavelet analysis). HHT is based on the Hilbert transform, a linear mathematical operator that takes each IMF $c_k(t)$ and produces a function $H[c_k](t)$ by convolution with the function $1/(\pi t)$

$$H[c_k](t) = \mathbb{P}\int_{-\infty}^{\infty} \frac{c_k(t')}{\pi(t-t')}dt', \tag{2}$$

where $\mathbb{P}$ indicates the Cauchy principal value. The application of the Hilbert transform to each IMFs allows the construction of an analytic function, $\tilde{c}_k(t) = c_k(t) + iH[c_k](t)$, so that the evolution of each IMFs can be represented in the plane $\mathcal{C} = \{c_k(t), H[c_k](t)\}$. Each point in the plane $\{c_k(t), H[c_k](t)\}$ can be also given using a polar representation $\mathcal{C} = \{A_k(t), \varphi_k(t)\}$, that is,

$$A_k(t) = \sqrt{c_k^2(t) + H[c_k]^2(t)}, \tag{3}$$

$$\varphi_k(t) = \tan^{-1}\left\{\frac{H[c_k](t)}{c_k(t)}\right\}, \tag{4}$$

where $A_k(t)$ is the instantaneous amplitude and $\varphi_k(t)$ is the instantaneous phase of the k-th empirical mode c_k. This polar representation allows the introduction of the instantaneous frequency, $f_k(t)$, which can be simply defined as

$$f_k(t) = \frac{1}{2\pi}\frac{d\varphi_k(t)}{dt}. \tag{5}$$

Generally, unless of intermittency phenomenon (Huang et al., 1998, 2009), the instantaneous frequency $f_k(t)$ of each IMF ranges over a limited frequency band so that it is possible to introduce a mean characteristic oscillation timescale τ_k of each IMF, which is defined as $\tau_k =< f_k(t) >^{-1}$, being $< \ldots >$ time average. As a result of the HHT method, each IMF is modulated both in amplitude and in frequency, which is a fundamental property to correctly characterize nonstationary time series, while the inherent adaptive character of the HHT method is suitable for investigating nonlinearities present in a time series (Huang et al., 1998).

From the concepts of instantaneous amplitude and frequency, the instantaneous energy content can be simply defined by means of the so-called Hilbert-Huang spectrum $H(f, t)$, enabling us to represent the amplitude

(or square amplitude, i.e., energy density) in a time-frequency plane and to derive local information on energy content of each IMF. By integrating over time, the marginal Hilbert power spectral density (PSD) $H(f)$ can be derived as

$$H(f) = \int_0^T \frac{H(f,t')}{f} dt', \tag{6}$$

which allows us to obtain global energy density distribution and to investigate spectral slopes and breaks (as for Fourier PSD). From both the Hilbert-Huang spectrum and the marginal Hilbert PSD, a measure of the intermittency character of time series (similar to the intermittency defined in the wavelet analysis) can be found by introducing the degree of stationarity $DS(f)$ as

$$DS(f) = \frac{1}{T}\int_0^T \left(1 - \frac{H(f,t')}{h(f)}\right)^2 dt', \tag{7}$$

with being $h(f) = \langle H(f)\rangle_T$ and T the length of the time series (see ; Consolini et al., 2017; Huang et al., 1998, for more details). If $DS(f) = 0$ the frequency component f is stationary, conversely if $DS(f) > 0$ the frequency component is nonstationary.

Both $H(f,t)$ and $H(f)$ have a totally different meaning from the Fourier spectral analysis. Indeed, the persistence of a purely wave component through the time series means that energy at a frequency f exists for Fourier analysis, while a higher likelihood for such a wave to have appeared locally means that energy exists at the frequency f for Hilbert analysis, since the Hilbert spectrum is a weighted not-normalized joint amplitude-(energy) frequency-time distribution (Huang et al., 2009, 1998).

Thus, the HHT approach is widely useful to carry out nonlinearities and/or nonstationarities embedded in time series with a completely adaptive behavior (Huang et al., 1998, 2009), although, as for each time series analysis method, some outstanding open problems need to be outlined as end effects and/or stopping criteria for the sifting process (see, e.g., Huang & Wu, 2008; Wu & Huang, 2009, for more details).

2.3. Correlation Dimension and K_2 Entropy

The behavior of a dynamical system, as the magnetosphere, can be examined by looking at the dimensionality of the phase-space (Ott, 1994). In particular, a dynamical system is usually defined *chaotic* if its dimension is a noninteger value (Falconer, 2005; Strogatz, 2018). The presence and degree of chaos can be quantified by using different measures as the correlation dimension and the K_2 entropy (Grassberger & Procaccia, 1983; Takens, 1981). These measures can be estimated by selecting an embedding dimension m and a time delay Δ to construct a m-component state vector from a time series $y(t)$ as

$$\mathbf{Y}_k = \{y_1(t_k), y_2(t_k), \ldots, y_m(t_k)\}, \tag{8}$$

where $y_l(t_k) = y(t_k + (l+1)\Delta)$. Then, the correlation integral is defined as

$$C(r,m) = \lim_{N\to\infty} \frac{1}{N^2} \sum_{i=1}^{N}\sum_{j=1}^{N} \Theta(r - |\mathbf{Y}_i - \mathbf{Y}_j|), \tag{9}$$

where Θ is the Heavyside step function, r is a threshold distance between two points in the phase-space, and N is the number of considered phase-space states. If $r \to 0$ the correlation integral will follow a power law behavior as $C(r,m) \sim r^{D_2}$, being D_2 the correlation dimension defined as

$$D_2 = \lim_{r\to 0} \frac{\log C(r,m)}{\log r}. \tag{10}$$

By increasing the embedding dimension m, the correlation dimension converges to its true value: if $D_2 = m$ the system explores the available phase-space, while when $D_2 < m$ a (strange) attractor is present. The correct choice of both m and Δ is crucial for a correct estimation of the correlation dimension (Takens, 1981). Usually, the time delay Δ is chosen as that corresponding to the first minimum of the autocorrelation function (often estimated by using delayed mutual information), while the embedding dimension m is chosen as the lowest value for which the correlation dimension converges to a constant value (Takens, 1981).

From the correlation integral, the K_2 entropy can be defined as

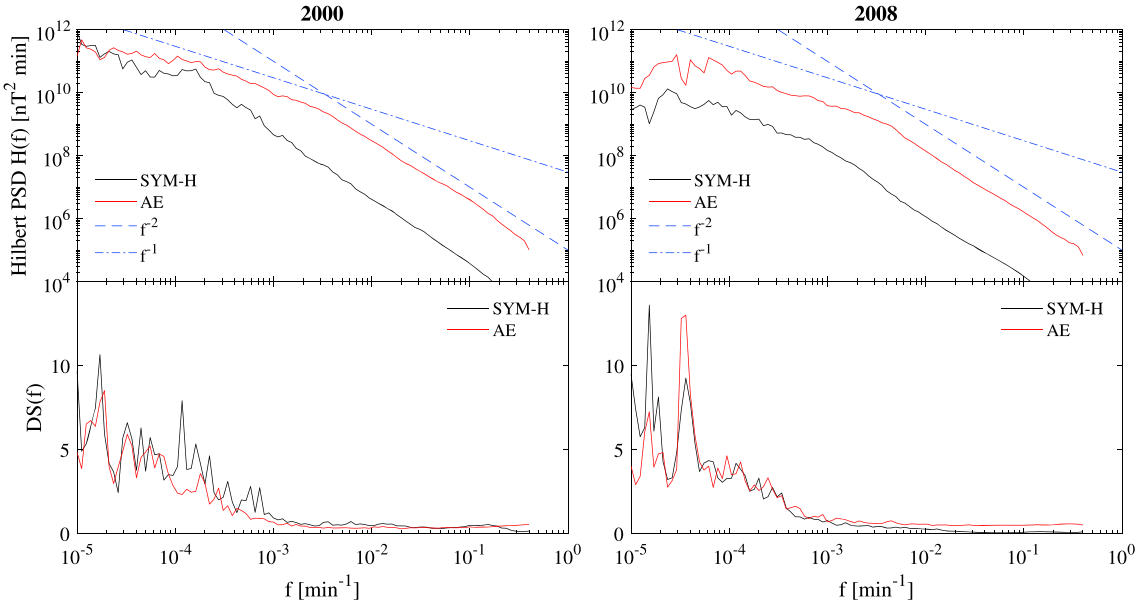

Figure 2. Marginal Hilbert PSD $H(f)$ and degree of stationarity $DS(f)$ of the time series during solar maximum (left panels) and minimum (right panels) phases. Black and red lines refer to SYM-H and AE indices, respectively, while both f^{-2} and f^{-1} are shown for reference. PSD = power spectral density; DS = degree of stationarity.

$$K_2 = \lim_{r\to 0} \frac{1}{\Delta t} \log \frac{C(r,m)}{C(r,m+1)}, \tag{11}$$

where Δt is the sampling rate. This entropy measures the rate of loss of information, since K_2^{-1} is the timescale over which the behavior of the system can be accurately predicted, as well as it is a measure of sensitivity of the system to changes in initial conditions (Grassberger & Procaccia, 1983). Both D_2 and K_2 are useful dimensions to distinguish between (deterministic) chaotic and (nondeterministic) random behavior: if K_2 is finite, the system is chaotic, while if $K_2 \to \infty$, the system is nondeterministic.

3. Results and Discussion

As a first step of our analysis we decompose the original signals into a set of IMFs (data not shown). This return a series of IMFs plus a residue, each of which characterized by a different characteristic timescale τ_k. In detail, we obtain in the case of AE 26 and 28 IMFs for the year 2000 and 2008, respectively, and 25 and 23 IMFs for the year 2000 and 2008, respectively, in the case of SYM-H index. The obtained number of IMFs is higher than what is expected in the case of a stochastic noise (as a random Brownian motion or a fractional noise) time series containing the same number of points, which should be ~19 IMFs, being the expected number approximately equals to $\#IMFs \simeq \ln_2 N_{points}$ (Flandrin et al., 2004). That suggests the existence of much more information in the AE and SYM-H time series than in a simple stochastic noise. Furthermore, the different number of IMFs obtained for the two selected periods gives us information on the changes of the complexity degree of the AE and SYM-H signals with the solar activity levels.

We initiate our discussion on the obtained results by analyzing the spectral features and the degree of stationarity (DS) of the two geomagnetic indices for the two selected time intervals. This is done using the Hilbert marginal PSD and the DS as defined in section 2.2.

The Hilbert marginal PSDs and the DS are reported for each selected period in Figure 2.

Despite the different activity level of geomagnetic disturbance between the two selected periods, the spectral features show only a limited number of differences. Similar spectral slopes and frequency break position are found both in the solar maximum and minimum phases. However, a clear difference is found between SYM-H and AE: the former has a frequency break at $f_b^{\text{SYM-H}} \sim 10^{-3} \div 10^{-4}$ min^{-1}, in agreement with previous findings (Wanliss & Showalter, 2006), while the latter has a frequency break at $f_b^{\text{AE}} \sim 4 \times 10^{-3}$ min^{-1} (Tsurutani et al., 1990). Moreover, low frequencies are characterized by a $\sim f^{-1}$ behavior, while a steeper slope is found for $f > f_b$ (i.e., $\sim f^{-2}$). The only significant change with the solar cycle phase is the increase in the range of frequencies

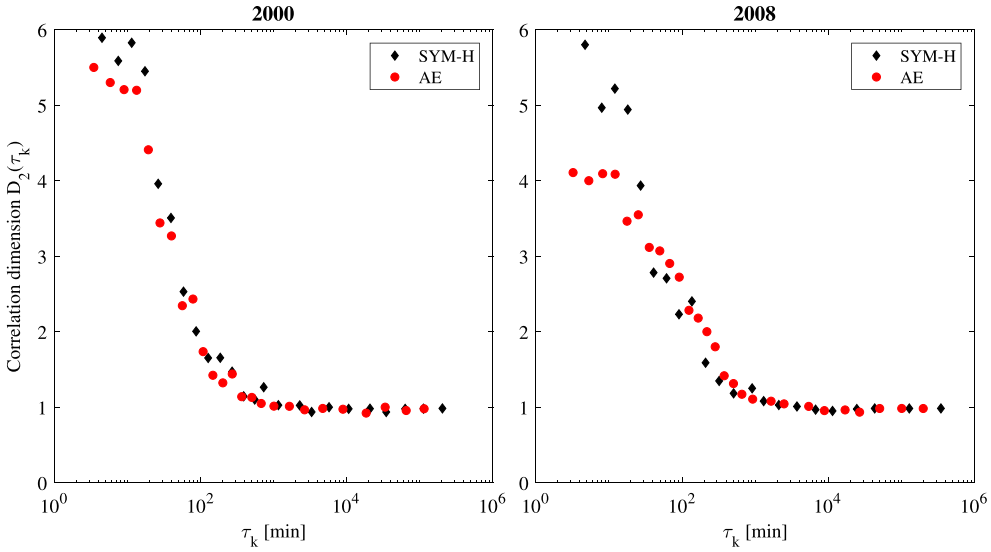

Figure 3. Scale-to-scale correlation dimension $D_2(\tau_k)$ for time series during solar maximum (left panels) and minimum (right panels) phases. Black diamonds refer to SYM-H index, while red circles are associated with AE index.

where a spectral range $\sim f^{-2}$ is observed. The $f^{-1} - f^{-2}$ spectral break moves to a lower frequency during the maximum phase of the solar activity cycle (the year 2000). That could be due to the existence of long time periods characterized by disturbed conditions in the SYM-H index, which are the consequence of a major number of geomagnetic storms characterized by a duration longer than 1 day. In terms of correlated noise, being the PSD related to the autocorrelation function, we can say that the correlation length extends during the maximum of the solar cycle, which corresponds to a major number of long duration storms.

By looking at the DS of both AE and SYM-H indices, we note that DS(f) $\sim$ 1 for $f > f_b$, that is, where the spectral features are characterized by a spectral slope −2. This result suggests that the high-frequency components of SYM-H and AE indices are nonstationary components with stationary increments of the fluctuations (A. Davis et al., 1994).

Since the EMD allows us to obtain empirical modes characterized by different mean oscillatory timescales (Huang et al., 1998), we are able to investigate dynamical system features following a scale-to-scale approach. That means to evaluate both the correlation dimension D_2 and the K_2 entropy for each IMF derived from equation (1) in order to characterize the features of the fluctuations at each characteristic timescale τ_k. We selected a time delay $\Delta = 200$ min, which corresponds to the first minimum of the autocorrelation function evaluated by using mutual information (see for details ; Alberti et al., 2017; De Michelis et al., 2011), although no significant variations can be found by using a different value (Vassiliadis et al., 1990), and an embedding dimension $m = 6$, for which a convergence value for both D_2 and K_2 is observed (Vassiliadis et al., 1990). Figure 3 reports the results obtained in the case of the correlation dimension $D_2(\tau_k)$ evaluated for each IMFs and according to the two different phases of the solar cycle.

The dimensionality of the system clearly exhibits a scale-dependent behavior characterized by a decrease in the values of $D_2(\tau_k)$ with the increase of the values of τ_k, and approaching to a constant value $D_2(\tau_k) \sim 1$ for $\tau_k \gtrsim 200$ min. This confirms previous results (see, e.g., Alberti et al., 2017; Consolini & De Michelis, 2005; Kamide & Kokubun, 1996) according to which the overall magnetospheric dynamics can be described as the result of a superposition of processes both purely internal (although externally triggered) and externally driven which work on different timescales. The former are generally characterized by the occurrence of coherent intermittent activity bursts (Consolini, 2002, 1997; Uritsky & Pudovkin, 1998) occurring on timescales smaller than 100 min, due to the internal processes related to the loading-unloading dynamics of the Earth's magnetotail (Consolini & De Michelis, 2005; Kamide & Kokubun, 1996), while the latter usually occur on longer timescales ($\tau \gtrsim 200$ min). We note that the short-timescale modes ($\tau_k < 200$ min) are characterized by high dimensionality, being $D_2(\tau_k) \gtrsim 2$. This suggests that the purely internal magnetospheric dynamics cannot be represented as a linear system, at least two (or more) variables are indeed necessary to completely describe the features on these timescales. Conversely, all the empirical modes having $\tau_k \gtrsim 200$ min are characterized by a correlation

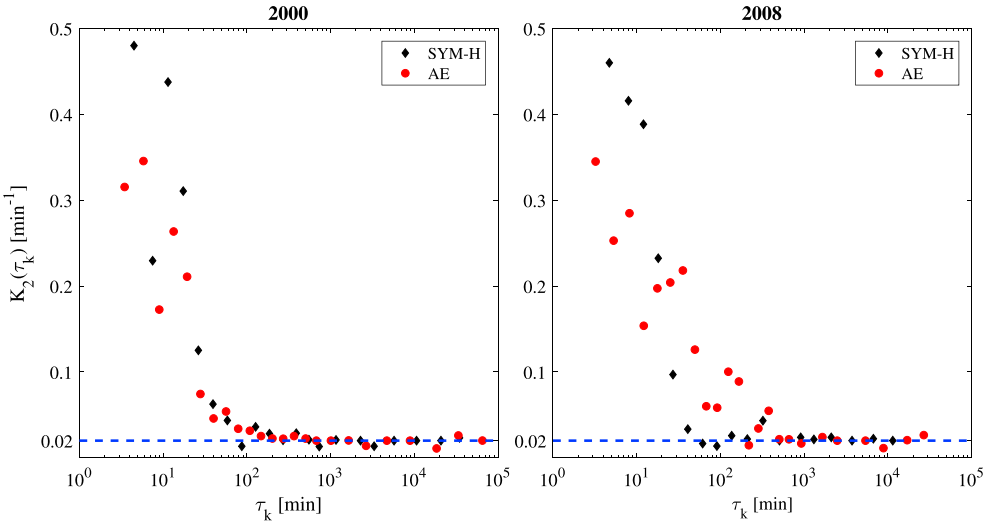

Figure 4. $K_2(\tau_k)$ entropy for time series during solar maximum (left panels) and minimum (right panels) phases. Black diamonds refer to SYM-H index, while red circles are associated with AE index. The dashed blue line corresponds to $K_2 = 0.02$ which is the convergence value for K_2 entropy.

dimension $D_2(\tau_k) \sim 1$, which suggests that the long-timescale magnetospheric dynamics can be described by using one system variable and that the observed changes can be well-reproduced by using interplanetary parameters on similar timescales (Alberti et al., 2017). Another interesting result is the quasi saturation of D_2 at timescale $\tau_k < 20$ min around values higher than 4. The observed behavior of $D_2(\tau_k)$ with the timescale suggests that dynamics of these indices at long and short timescales is characterized by completely different dynamical processes. For instance, AE index is characterized by a correlation dimension $D_2(\tau_k) \simeq 1$ at timescales longer than 1000 min and by a correlation dimension $D_2(\tau_k) \sim 4 \div 5$ at timescales below 20 min. This result suggests the presence of a topological phase transition (Chang et al., 1992, 2003) being the short and long timescales associated with completely different dynamical features as stressed by the correlation dimension D_2.

Another interesting result is the continuous change of the correlation dimension $D_2(\tau_k)$ in the range of timescales from $\tau_k = 20$ min to $\tau_k = 1000$ min, which suggests that a single correlation dimension is not capable of describing the complexity features of the AE and SYM-H time series. The behavior of $D_2(\tau_k)$ can be interpreted as the evidence of a phenomenon analogous to the intermittency observed in the case of turbulence where a hierarchy of dimensions is necessary to describe the complex nature of the dissipation field. In other words, this is the temporal counterpart of the multifractal nature of such indices (Consolini et al., 1996). In this framework, the value of $D_2 = 3.6$ found by Vassiliadis et al. (1990) has to be interpreted as an overall effective correlation dimension, a sort of mean value.

Taking into consideration these forecast horizon results, we can conclude that, for forecasting purposes, modeling short-term variations is more complex than reproducing long-term variations. We will return on this point in the next section when we discuss the possible implication of our results in the framework of Space Weather forecasting.

A similar scale-behavior is found by analyzing the K_2 Kolmogorov entropy which decreases as τ_k increases, approaching to a convergence value of $K_2 = 0.02$ min^{-1}. Figure 4 shows the behavior of $K_2(\tau_k)$ with the characteristic timescale τ_k for the two geomagnetic indices and the two different phases of solar cycle. This suggests that the forecast horizon changes with the scale, moving from a minimum value of ∼2 min up to ∼50 min. For this reason the large-timescale modes are characterized by a forecast horizon which is higher than that associated with the short-timescale modes. This means that the forecast of purely internal processes is more difficult than that of externally driven ones. We note that the behavior of both D_2 and K_2 are independent on solar activity and are well in agreement with previous findings (see, e.g., Vassiliadis et al., 1990) where a correlation dimension D_2 of ∼3.6 and a entropy K_2 of ∼0.2 min^{-1} were found by considering the raw data of AE index. The main novelty introduced here is that we find a dependence on the timescale at which a particular

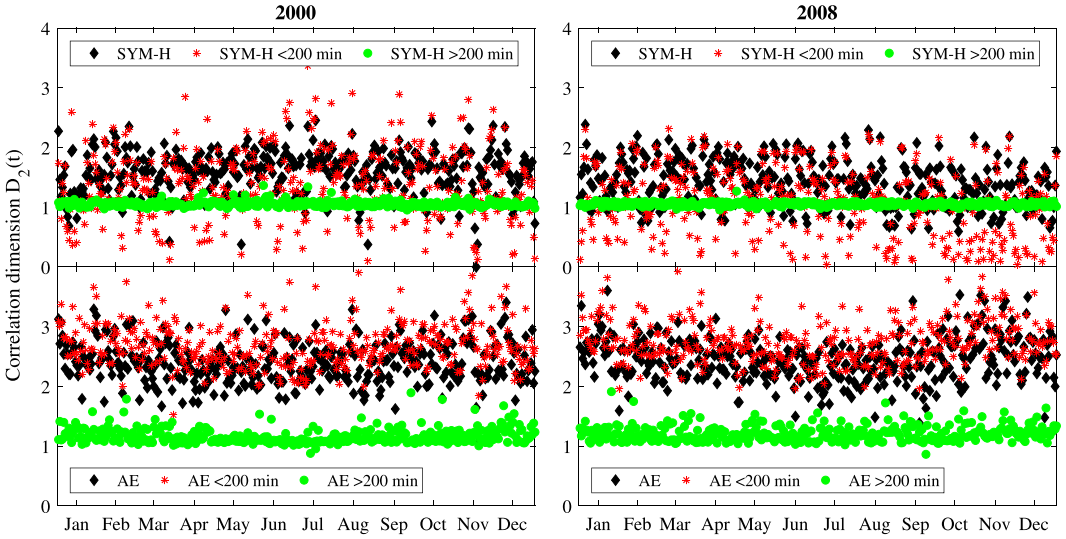

Figure 5. Daily correlation dimension D_2 for time series during solar maximum (left panels) and minimum (right panels) phases. Upper and lower panels refer to SYM-H and AE, respectively. Black diamonds refer to the raw data, red asterisks to short-term (τ_k < 200 min) reconstructions, and green circles to long-term (τ_k > 200 min) ones, respectively.

process can operate for both analyzed quantities, confirming that there is a clear emergence of a separation of the timescales between processes with have different origin (Alberti et al., 2017).

It has been suggested by Vassiliadis et al. (1990) that the correlation dimension is independent of the geomagnetic activity level, for this reason we have decided to investigate this aspect. Since dynamical system properties dramatically change with the scale τ_k we use the same approach introduced by Alberti et al. (2017) to separate in the time series of the geomagnetic indices the short-term variations (i.e., τ < 200 min) from long-term ones (i.e., $\tau \gtrsim$ 200 min) and successively we evaluate D_2 and K_2 for both the short-term and long-term reconstructions in order to examine their dependence on the geomagnetic activity level. D_2 and K_2 are evaluated for each day of the year (i.e., on time series of length 1,440 points) in order to include both the quiet and disturbed periods, without operating a separation in terms of geomagnetic indices values. The

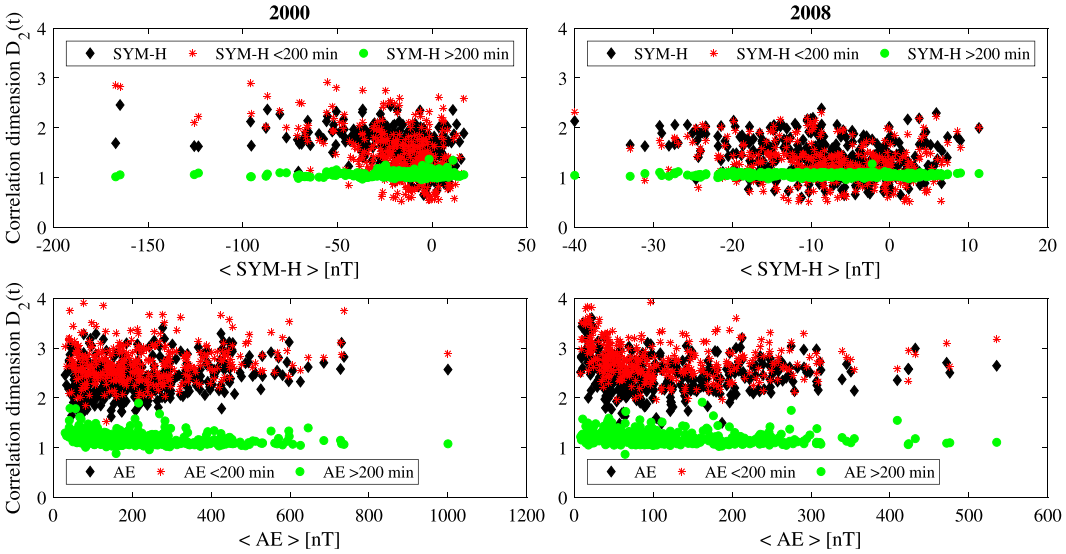

Figure 6. The dependence of the daily correlation dimension D_2 as a function of the daily value of AE and SYM-H indices during solar maximum (left panels) and minimum (right panels) phases. Upper and lower panels refer to SYM-H and AE, respectively. Black diamonds refer to raw data, red asterisks to short-term (τ_k < 200 min) reconstructions, and green circles to long-term (τ_k > 200 min) ones, respectively.

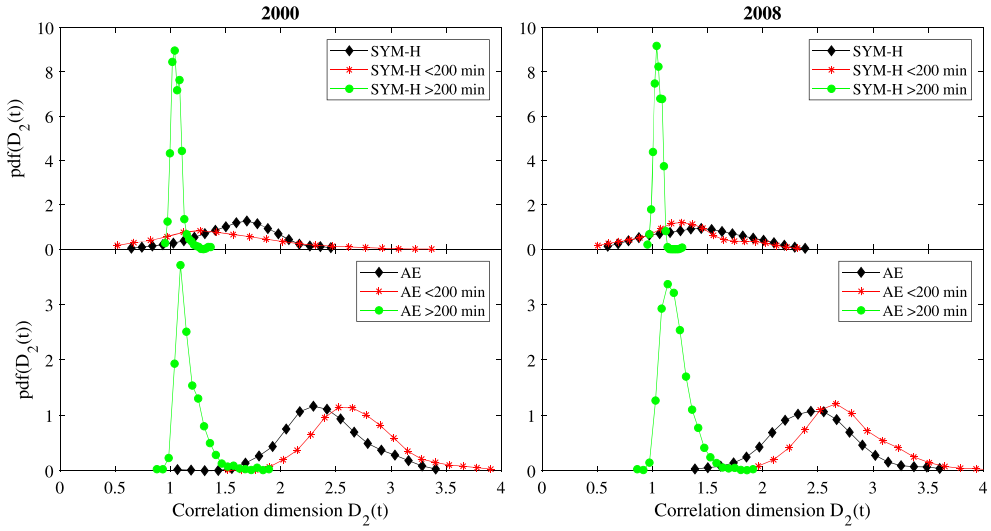

Figure 7. The pdfs of daily correlation dimension for time series during solar maximum (left panels) and minimum (right panels) phases. Upper and lower panels refer to SYM-H and AE, respectively. Black diamonds refer to raw data, red asterisks to short-term (τ_k < 200 min) reconstructions, and green circles to long-term (τ_k > 200 min) ones, respectively. pdf = Probability distribution function.

daily correlation dimensions for raw daily data and the corresponding long- and short-term reconstructions are shown in Figure 5 according to the maximum and minimum phases of the solar cycle.

We note that the daily D_2 for long-term reconstruction does not show a sensible dependence on the geomagnetic activity level, while D_2 of raw data and short-term reconstruction display a certain spread over a wide range of values and exhibit a small dependence on the geomagnetic activity level (see Figure 6). In particular, during the solar maximum the correlation dimension of the short-term (τ_k < 200 min) reconstruction of both AE and SYM-H seems to increase with the daily geomagnetic disturbance, measured in terms of daily value of AE and SYM-H (⟨AE⟩ and ⟨SYM-H⟩). During the solar minimum the daily correlation dimension of SYM-H is nearly constant, while that associated with AE shows an increase as a function of the daily value of AE. A large spreading of the D_2 is observed during nearly quiet conditions in both the two solar phases and for both the two geomagnetic indices.

Similar conclusions can be drawn by investigating the probability distribution functions (pdfs) of the daily correlation dimension for short-term and long-term reconstructions, and raw data as well. Figure 7 shows the pdfs of the daily correlation dimension for the two reconstructions and the raw data. As already noted, it can be argued that a lower sensitive variation is found for the long-term reconstruction whose pdf is centered around ∼1 with small variations (between 0.8 and 2) in the case of both SYM-H index and AE index regardless of the phases of solar cycle. A wider range of variability is found when short-term reconstructions are considered with a clear difference between SYM-H and AE: the former is characterized by a mean value of $D_2 \sim 1.5 - 2$, while the latter shows a higher value (i.e., $D_2 \sim 2.5 - 3$) during both phases of the solar cycle. This means that forecasting short-term SYM-H behavior is less complex than forecasting short-term AE behavior because of less parameters are required to describe the dynamical changes on these timescales.

4. Summary and Conclusions

The aim of the present study was to examine the scale-to-scale forecast horizon of magnetospheric dynamics. The analysis was based on the investigation of the correlation dimension D_2 and Kolmogorov entropy K_2 of the fluctuations of two different geomagnetic indices, AE and SYM-H, which are usually used as proxies of the overall magnetospheric dynamics in response to the solar wind and the interplanetary medium changes. By applying the EMD method to the selected geomagnetic indices time series, we analyzed the different IMFs in which each selected time series can be decomposed and related each mode to a mean characteristic oscillation timescale. In this way, we evaluated the correlation dimension D_2 and Kolmogorov entropy K_2 scale-to-scale trying to identify and characterize, through the behavior of these two physical quantities, the

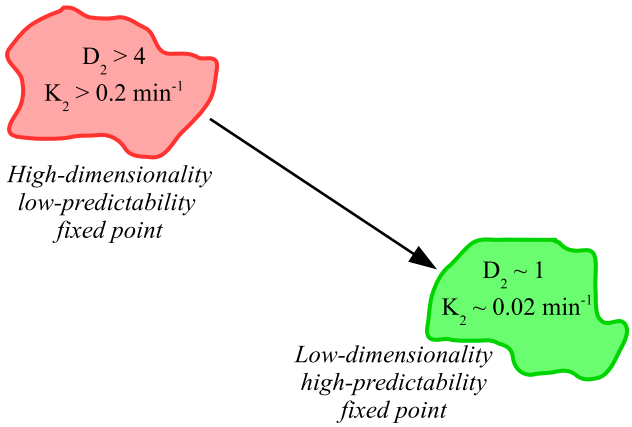

Figure 8. A sketch of the D_2 and K_2 evolution with timescales.

different processes responsible for the observed fluctuations at the different timescales. The main results of our analysis can be summarized as follows:

- The correlation dimension $D_2(\tau_k)$ shows a clear dependence on the timescales τ_k. $D_2(\tau_k)$ rapidly increases with decreasing τ_k from a value $D_2(\tau_k) \sim 1.0$, at timescales above $\tau_k > 200$ min, to $D_2(\tau_k) \sim 4.0 \div 6.0$, at timescales $\tau_k < 20$ min, where it tends to saturate. This behavior is common for AE and SYM-H regardless of the solar activity level;
- The Kolmogorov entropy $K_2(\tau_k)$ shows a behavior analogous to that of the correlation dimension, indicating that below 200 min the forecast horizon rapidly decreases reaching values of the order of few minutes (~2 min);
- The daily correlation dimension D_2 both for the short-term ($\tau_k < 200$ min) and long-term ($\tau_k > 200$ min) reconstructions of the two geomagnetic indices shows a different dependence on the geomagnetic activity level. In particular, the long-term reconstruction displays a value of $D_2 \sim 1$ regardless of the geomagnetic activity level, while the D_2 relative to the short-term reconstruction displays a larger value which slightly increases with the level of the geomagnetic disturbance.

The observed behavior of the correlation dimension D_2 as a function of the timescale τ_k may be explained by the fact that the dynamical properties of short- and long-timescale fluctuations have a different physical origin. Therefore, it seems that the long- and short-timescale fluctuations dynamics are governed by different fixed points, characterized by a different number of degrees of freedom (nearly 1 at long timescales and more than 4 at short timescales) and by a different forecast horizon (>50 min at long timescales and ~2 min at short ones). Figure 8 shows a sketch of the observed behavior. The emerging scenario from the scale-to-scale analysis of correlation dimension D_2 and Kolmogorov entropy K_2 is that in presence of a sort of topological continuous phase transition for the fluctuations at different timescales (Chang et al., 1992, 2003), being the fluctuations at timescales of the order of few minutes characterized by a completely different forecast horizon. Furthermore, we note that the ~200 min fluctuation timescale where the correlation dimension D_2 start to rapidly increase is well in agreement with the one below which the magnetospheric dynamics shows a nonlinear response to external driving as found in the seminal work by Tsurutani et al. (1990).

Different studies indicate that the overall magnetospheric dynamics is the result of the superposition of directly driven and loading-unloading processes (see, e.g., Consolini & De Michelis, 2005; Kamide & Kokubun, 1996, and references therein), where the former is mainly related to the plasma convection inside the magnetosphere and the latter to the transient activity and the impulsive energy releases occurring in the CPS tail region (Angelopoulos et al., 1996; Lui et al., 1998; Sharma et al., 2008). The plasma convection process, which enhances during periods of southward interplanetary magnetic field orientation, is a large-scale phenomenon that can be reasonable associated with a slow dynamics, conversely a fast turbulent dynamics characterizes the impulsive energy releases occurring in the tail CPS region (Vörös et al., 2006). These impulsive energy releases, which manifest in terms of auroral blobs and bursty-bulk-flows (Angelopoulos et al., 1996; Lui et al., 1998; Uritsky et al., 2002), present a quasi-critical nature as suggested by the distribution functions of both their sizes and time durations, which are characterized by scale-invariance (Angelopoulos et al., 1999; Consolini, 2002; Uritsky et al., 2002). Furthermore, it is now well established from a wide variety of studies that the plasma in the CPS and in the tail neutral sheet is in a turbulent state (see, e.g., Borovsky et al., 1997; Vörös et al., 2004, and references therein). On the basis of these observations, we can suggest that the different character of the short- and long-timescale fluctuations in terms of correlation dimension (i.e., dimensionality of the underlined process) and Kolmogorov entropy is the fingerprint of turbulent energy releases related to the unloading mechanisms and the plasma convection, respectively.

The findings reported here shed new light on the framework of Space Weather forecasting. The present study indicates that it is possible to correctly forecast the geomagnetic response to the solar wind changes at timescales longer than 1 hr using some proxies of the solar wind and IMF conditions. Many recent studies, for example, those based on ANNs, support this finding. Indeed, different models, which are capable of forecasting the hourly Dst index using quantities associated with the solar wind and interplanetary magnetic field conditions (magnetic field components, solar wind parameters, etc.), have been developed. Conversely, the

forecasting of short-timescale fluctuations seems to be more difficult due to the higher number of degrees of freedom involved and to the very short forecast horizon (∼2 min), which would require to get information on the fast dynamics of the tail regions.

One of the more significant findings to emerge from this study is that it is quite reasonable to get a good forecast of that part of the magnetospheric dynamics associated with the enhancement convection processes using solar wind and interplanetary magnetic field measurements, , while the fast dynamics associated with the unloading mechanisms taking place in the CPS and neutral sheet tail regions requires a deeper knowledge of the magnetospheric tail conditions. Considerably, more work will need to be done to determine some proxies for the tail dynamical state with a time resolution of seconds, necessary to overcome complications associated with the forecasting of short-timescale dynamics. The individuation and the construction of a proxy for the internal fast dynamics should be considered as a must, being the short-timescale changes responsible for a lot of phenomena such as the generation of the large ground-induced currents due to the rapid intensification and variability of magnetospheric and ionospheric current systems driven by major geomagnetic storms. Space Weather associated ground-induced currents pose a serious threat to the reliability of power-transmission systems and other electrically conducting infrastructures such as oil and gas pipelines.

Further research is required to better characterize the features of short-timescale fluctuations of geomagnetic indices and this will be the subject of future works.

Acknowledgments
The authors acknowledge and thank the staff of Space Physics Data Facility, NASA/Goddard Space Flight Centre, who arranged and made freely available the OMNI2 data, that are used in this work. The data have been downloaded from http://omniweb.gsfc.nasa.gov/ow.html. The authors also acknowledge World Data Center for Geomagnetism (Kyoto) for the use of the geomagnetic indices data. All the derived data products presented in this paper are available upon request by email to the corresponding author (giuseppe.consolini@inaf.it).

References

Ahn, B. H., Akasofu, S. I., & Kamide, Y. (1983). The Joule heat-production rate and the particle energy injection rate as a function of the geomagnetic indices AE and AL. *Journal of Geophysical Research*, *88*, 6275.

Alberti, T., Consolini, G., Lepreti, F., Laurenza, M., Vecchio, A., & Carbone, V. (2017). Timescale separation in the solar wind-magnetosphere coupling during St. Patrick's Day storms in 2013 and 2015. *Journal of Geophysical Research: Space Physics*, *122*, 4266–4283. https://doi.org/10.1002/2016JA023175

Angelopoulos, V., Coroniti, F. V., Kennel, C. F., Kivelson, M. G., Walker, R. J., Russell, C. T., et al. (1996). Multi-point analysis of a BBF event on April 11, 1985. *Journal of Geophysical Research*, *101*, 4967–4989.

Angelopoulos, V., Mukai, T., & Kokubun, S. (1999). Evidence for intermittency in Earth's plasma sheet and implications for self-organized criticality. *Physics of Plasmas*, *6*, 4161.

Baker, D. N., Klimas, A. J., McPherron, R. I., & Büchner, J. (1990). The evolution from weak to strong geomagnetic activity: An interpretation in terms of deterministic chaos. *Geophysical Research Letters*, *17*, 41–43.

Balasis, G., Daglis, I. A., Kapiris, P., Mandea, M., Vassiliadis, D., & Eftaxias, K. (2006). From pre-storm activity to magnetic storms: A transition described in terms of fractal dynamics. *Annales Geophysicae*, *24*, 3557–3567.

Borovsky, J. E. (2013). Canonical correlation analysis of the combined solar wind and geomagnetic index data sets. *Journal of Geophysical Research: Space Physics*, *119*, 5364–5381. https://doi.org/10.1002/2003JAO19607

Borovsky, J. E., Elphic, R. C., Funsten, H. O., & Thomsen, M. F (1997). The Earth's plasma sheet as a laboratory for flow turbulence in high−β MHD. *Journal of Plasma Physics*, *57*, 1–34.

Chang, T., Tam, S. W. Y., Wu, C.-C., & Consolini, G. (2003). Complexity, forced and/of self-organized criticality and topological phase transitions in space plasmas. *Space Science Reviews*, *107*, 425–445.

Chang, T., Vvedensky, D. D., & Nicoll, J. F. (1992). Differential renormalization-group generators for static and dynamic critical phenomena. *Physics Reports*, *217*, 279.

Consolini, G. (1997). Sandpile cellular automata and the magnetospheric dynamics. In S. Aiello (Ed.), *Cosmic physics in the year 2000* (pp. 123). Bologna: SIF.

Consolini, G. (2002). Self-organized criticality: A new paradigm for the magnetotail dynamics. *Fractals*, *10*, 275–283.

Consolini, G. (2018). Emergence of dynamical complexity in the Earth's magnetosphere. In E. Camporeale, S. Wing, & J. R. Johnson (Eds.), *Machine learning techniques for space weather* (pp. 177–202). Amsterdam, Netherlands: Elsevier.

Consolini, G., Alberti, T., Yordanova, E., Marcucci, M. F., & Echim, M. (2017). A Hilbert-Huang transform approach to space plasma turbulence at kinetic scales. *Journal of Physics: Conference Series*, *900*, 12003.

Consolini, G., & De Michelis, P. (2005). Local intermittency measure analysis of AE index: The directly driven and unloading component. *Geophysical Research Letters*, *32*, L05101. https://doi.org/10.1029/2004GL022063

Consolini, G., Marcucci, M. F., & Candidi, M. (1996). Multifractal structure of auroral electrojet index data. *Physical Review Letters*, *76*, 4082–4085.

Davis, A., Marshak, A., Wiscombe, W., & Cahalan, R. (1994). Multifractal characterizations of nonstationarity and intermittency in geophysical fields: Observed, retrieved, or simulated. *Journal of Geophysical Research*, *99*, 8055–8058. https://doi.org/10.1029/94JD00219

Davis, T., & Sugiura, M. J. (1966). Auroral electrojet activity index AE and its universal time variations. *Journal of Geophysical Research*, *71*, 785–791.

De Michelis, P., Consolini, G., Materassi, M., & Tozzi, R. (2011). An information theory approach to the storm-substorm relationship. *Journal of Geophysical Research*, *116*, A08225. https://doi.org/10.1029/2011JA016535

De Michelis, P., Consolini, G., & Tozzi, R (2012). On the multi-scale nature of large geomagnetic storms: An empirical mode decomposition analysis. *Nonlinear Processes in Geophysics*, *19*, 667–673.

Falconer, K. (2005). *Fractal geometry: Mathematical foundations and applications* (2nd ed.). Chichester, UK: Wiley. https://doi.org/10.1002/0470013850

Flandrin, P., Rilling, G., & Goncalvés, P. (2004). Empirical mode decomposition as a filter bank. *IEEE Signal Processing Letters*, *11*, 112–114.

Grassberger, P., & Procaccia, I. (1983). Characterization of strange attractors. *Physical Review Letters*, *50*, 346.

Huang, N. E., Shen, Z., Long, S. R., Wu, M. L. C., Shih, H. H., Zheng, Q. N., et al. (1998). The empirical mode decomposition and the Hilbert spectrum for nonlinear and non-stationary time series analysis. *Proceedings of the Royal Society of London A*, *454*, 903–995.

Huang, N. E., & Wu, Z. (2008). A review on Hilbert-Huang transform: Method and its applications to geophysical studies. *Reviews of Geophysics*, *46*, RG2006. https://doi.org/10.1029/2007RG000228

Huang, N. E., Wu, Z., Long, S. R., Arnold, K. C., Chen, X., & Blank, K (2009). On instantaneous frequency. *Advances in Data Science and Adaptive Analysis*, *1*, 177–229.

Iyemori, T. (1990). Storm-time magnetospheric currents inferred from midlatitude geomagnetic field variations. *Journal of Geomagnetism and Geoelectricity*, *42*, 1249.

Kamide, Y., & Kokubun, S. (1996). Two-component auroral electrojet: Importance for substorm studies. *Journal of Geophysical Research*, *101*, 089.

Klimas, A. J., Vassiliadis, D., Baker, D. N., & Roberts, D. A (1996). The organised nonlinear dynamics of the magnetosphere. *Journal of Geophysical Research*, *101*, 13089.

Lui, A. T. Y., Chapman, S. C., Liou, K., Newell, P. T., Meng, C. I., Brittnacher, M., & Parks, M. (2000). Is the dynamic magnetosphere an avalanching system? *Geophysical Research Letters*, *27*, 911–914.

Lui, A. T. Y., Liou, K., Newell, P. T., Meng, C.-I., Ohtani, S.-I., Ogino, T., et al. (1998). Plasma and magnetic flux transport associated with auroral breakups. *Geophysical Research Letters*, *25*, 4059–4062.

Ott, E. (1994). *Chaos in dynamical systems*. New York: Cambridge University Press.

Pallocchia, G., Amata, E., Consolini, G., Marcucci, M. F., & Bertello, I. (2008). AE index forecast at different time scales through an ANN algorithm based on L1 IMF and plasma measurements. *Journal of Atmospheric and Solar-Terrestrial Physics*, *70*, 663–668.

Sharma, A. S. (1995). Assessing the magnetosphere's nonlinear behavior: Its dimensional is low, its predictability is high. *Reviews of Geophysics*, *33*, 645–650.

Sharma, A. S., Nakamura, R., Runov, A., Grigorenko, E. E., Hasegawa, H., Hoshino, M., et al. (2008). Transient and localized processes in the magnetotail: A review. *Annales Geophysicae*, *26*, 955–1006.

Sharma, A. S., Sitnov, M. I, & Papadopoulos, K. (2001). Substorms as nonequilibrium transitions of the magnetosphere. *Journal of Atmospheric and Solar-Terrestrial Physics*, *63*, 1399.

Sitnov, M. I., Sharma, A. S., Papadopoulos, K., Vassiliadis, D., Valdivia, J. A., Klimas, A. J., & Baker, D. N. (2000). Phase transition-like behavior of the magnetosphere during substorms. *Journal of Geophysical Research*, *105*, 12955–12974.

Strogatz, S. (2018). *Nonlinear dynamics and chaos*. Boca Raton: CRC Press.

Takalo, J., & Timonen, J. (1997). Neural network prediction of AE data. *Geophysical Research Letters*, *27*, 2403–2406.

Takens, F. (1981). Detecting strange attractors in turbulence. In D. A. Rand & L.-S. Young (Eds.), *Lecture notes in mathematics* (vol. 898, pp. 366). Berlin: Springer.

Tsurutani, B., Sugiura, M., Iyemori, T., Sugiura, M., Iyemori, T., Goldstein, B. E., et al. (1990). The nonlinear response of AE to the IMF B_s driver: A spectral break at 5 hours. *Geophysical Research Letters*, *17*, 279–282. https://doi.org/10.1029/GL017i003p00279

Uritsky, V. M., Klimas, A. J., & Vassiliadis, D. (2001). Comparative study of dynamical critical scaling in the auroral electrojet index versus solar wind fluctuations. *Geophysical Research Letters*, *28*, 3809–3812.

Uritsky, V. M., Klimas, A. J., Vassiliadis, D., Chua, D., & Parks, G. (2002). Scale-free statistics of spatiotemporal auroral emissions as depicted by POLAR UVI images: The dynamic magnetosphere is an avalanching system. *Journal of Geophysical Research*, *107*, 1426.

Uritsky, V. M., & Pudovkin, M. I. (1998). Low frequency $1/f$-like fluctuations of the AE-index as a possible manifestation of self-organized criticality in the magnetosphere. *Annales Geophysicae*, *16*, 1580.

Vassiliadis, D. V., Sharma, A. S., Eastman, T. E., & Papadopoulos, K. (1990). Low-dimensional chaos in magnetospheric activity from AE time series. *Geophysical Research Letters*, *17*, 1841–1843.

Vörös, Z., Baumjohann, W., Nakamura, R., Runov, A., Zhang, T. L., Eichelberger, H. U., et al. (2004). Magnetic turbulence in the plasma sheet. *Journal of Geophysical Research*, *109*, A11215. https://doi.org/10.1029/2004JA010404

Vörös, Z., Baumjohann, W., Nakamura, R., Volwerk, M., & Runov, A. (2006). Bursty bulk flow driven turbulence in the Earth's plasma sheet. *Space Science Reviews*, *122*, 306–311.

Wanliss, J. A., & Showalter, K. M. (2006). High-resolution global storm index: Dst versus SYM-H. *Journal of Geophysical Research*, *111*, A02202. https://doi.org/10.1029/2005JA011034

Wei, H. L., Billings, S. A., & Balikhin, M. (2004). Analysis of geomagnetic activity of Dst index and self-affine fractals using wavelet transforms. *Nonlinear Processes in Geophysics*, *11*, 303–312. https://doi.org/1607-7946/npg/2004-11-303

Wu, Z., & Huang, N. E. (2009). Ensemble empirical mode decomposition: A noise-assisted data analysis method. *Advances in Adaptive Data Analysis*, *1*, 1–41.